Mol. Cells *30*, 533-543, December 31, 2010
DOI/10.1007/s10059-010-00151-7

Molecules and Cells



# Comparative Phenotypic and Physiological Characteristics of Spotted Leaf 6 *(spl6*) and Brown Leaf Spot2 (*bl2*) Lesion Mimic Mutants (LMM) in Rice

**Mohammad Nurul Matin, Saifullah Ahmed Saief, Mohammad Mominur Rahman, Dong Hoon Lee[1], Hoduck Kang[2], Dong Sun Lee[3], and Sang Gu Kang***

**Spontaneous necrotic lesions were found in a lesion mimic mutant brown leaf spot 2 (*bl2*) without pathogenic infection. Small spots in the seedlings appeared at the four leaves stage and gradually grew into a large round and black area with a gray center on the leaf surfaces. Lower growth habit and lower agronomic trait values with reduced stature, tiller, and panicle number, as well as lower yield potential were noted in the mutants relative to the trait values of the wild-type plants. Microscopic analysis revealed that mesophyll chloroplast was severely damaged or absent in the spotted area of the mutant leaves. Total chlorophyll content, hydrogen peroxide level, and catalase activity were increased at up to 45 days after germination and were dropped at 60 d in the mutant leaves. However, the total protein contents were reduced slightly with a growth period of up to 45 days and were increased at 60 days after germination. A gradual increment of the total ascorbic acid contents in the mutants were observed with advanced plant age, but increased until 45 days and dropped comparatively at 60 days in the wild-type leaves. Increased gene transcriptions of *OsPDI* and *OsGPX1* were noted in the spotted leaves as compared to the non-spotted leaves of the mutant and wild-type leaves, whereas transcripts of *OsTPX* were transcribed at lower levels in the spotted leaves as compared to the non-spotted leaves. The genetic nature of the *bl2* mutant indicated that the $F_1$ plants evidenced the wild-type phenotype and that *bl2* was governed by a single recessive gene.**

## INTRODUCTION

Rice mutants expressing spots on the leaf surface resembling disease symptoms in the absence of pathogen attack are referred to as lesion mimic mutant (LMM) (Balague et al., 2003; Dietrich et al., 1994; Gray et al., 2002). Throughout the life cycle, plants are exposed to a variety of biotic and abiotic stresses. To protect against stresses, they generate stress elicitors via metabolic and structural adjustments (Dietrich et al., 1994; Yamanouchi et al., 2002). The hypersensitive response (HR) is one of the mechanisms underlying protection against pathogen attack, in which plants kill their own cells around the invasion area, thus protecting against foreign agents and further pathogenic spread (Lam et al., 2001; Mittler et al., 1997). However, the cell death phenotype of LMMs is similar to the HR phenomena. In fact, LMM symptoms induce cell death in plants, resulting in the formation of lesions on the leaves, which is a programmed cell death process that has been previously described in many organisms (Kang et al., 2007; Tsunezuka et al., 2005). This cell death behavior has been programmed in the rice genome to occur spontaneously, mimicking modes of plant protection against stresses; this phenomenon is referred to as lesion resembling disease (*lrd*), and produces spots on the leaves without any type of pathogenic infection.

Lesion formation induced by cell death in the leaves is due primarily to defense responses triggered by pathogens that control the hypersensitive response (Greenberg et al., 1994; Morel and Dangl, 1997). Moreover, the involvement of several stresses, such as high light intensity as well as temperatures unsuited to plants have been recognized as triggers of and regulators of phenotypic expression in the LMMs (Bouchez et al., 2007; Dietrich et al., 1994; Matin et al., 2010; Noutoshi et al., 2006; Yamanouchi et al., 2002).

Lesion development in lesion mimic mutants has been previously described in many organisms, including rice (Kang et al., 2007; Liu et al., 2004; Matin et al., 2006; 2010; Mizobuchi et al., 2002; Mori et al., 2007; Qiao et al., 2010; Wu et al., 2008), Arabidopsis (Dietrich et al., 1994; Mosher et al., 2010; Noutoshi et al., 2006), barley (Buschges et al., 1997; Persson et al., 2009; Rostoks et al., 2006), maize (Hoisington et al., 1982; Johal et al., 1995; Simmons et al., 1998), and wheat (Sugie et al., 2007). Most of the LMM genes described thus far have been shown to control specific functions to regulate resistance mechanisms, some of which include ion channels (Balague et al.,

Molecular Genetics Laboratory, School of Biotechnology, Yeungnam University, Gyeongsan 712-749, Korea, [1]National Institute of Horticultural and Herbal Science, RDA, Jeju 697-943, Korea, [2]Department of Biological and Environmental Science, College of Life Science and Biotechnology, Dongguk University, Seoul 100-715, Korea, [3]Key Laboratory of Agro-Biodiversity and Pest Management of Education Ministry, Yunnan Agricultural University, Kunming 650201, China
*Correspondence: kangsg@ynu.ac.kr

Received June 15, 2010; revised August 15, 2010; accepted September 13, 2010; published online November 23, 2010

**Keywords:** *bl2,* catalase, lesion mimic mutant, *Oryza sativa*, *spl6*

2003), zinc-finger protein (Dietrich et al., 1997), heat shock protein (Yamanouchi et al., 2002), U-Box domain containing protein (Zeng et al., 2004), and clathrin-associated adaptor protein (Qiao et al., 2010). Some other genes have been implicated in the biosynthetic pathway (Brodersen et al., 2002; Ishikawa et al., 2001). More than 12 genes controlling the lesion mimic phenotype have been identified thus far (Buschges et al., 1997).

Although several LMM mutants that induce lesion formation have been identified thus far, little is currently known regarding the genetic, developmental, physiological, and phenotypic properties of each individual mutant of the LMM family. In this study, we describe a specific *bl2* mutant of rice LMMs. In an effort to gain greater insights into the mechanisms underlying lesion expression and the gene causative of the *bl2* phenotype, it is first necessary to understand the phenotypic characteristics. Therefore, we described herein the comparative phenotypic characteristics between naturally grown *bl2* and *spl6* mutants. Specifically, patterns of lesion formation, genetic segregation, agronomic characteristics, and the morphological and physiological properties of spot formation in the *bl2* mutant have been recorded and discussed. Thus, we have suggested herein that the rice *bl2* mutant may prove a useful material for investigation of the underlying nature of disease resistance and antioxidative stress in plants.

## MATERIALS AND METHODS

### Plant materials

Ethyl methane sulfonate (EMS)-induced rice lesion mimic mutant plants *bl2, spl6,* and wild type rice Milliang 23 (an *indica* cultivar) were employed for the experiments conducted herein. The rice plants were grown in a natural environment at a temperature between 30°C to 35°C in a paddy field in Yeungnam University, Gyeongsan, Korea. One month-old seedlings, grown in a greenhouse were transplanted in the field.

### Genetic analysis

To assess the inheritance pattern of the *bl2* mutant, hybrid crosses were generated between the *bl2* mutant (*indica* type) and Ilpoombyeo (*japonica* type) as well as *bl2* and Milliang 23 (*indica* type). The resultant $F_1$ seeds were cultivated in the greenhouse and were allowed to self-pollinate, thus generating a large population of $F_2$ progenies. Both of the parental types and $F_2$ progenies derived from *bl2* crossed with Ilpoombyeo and *bl2* crossed with Milliang 23 were transplanted in the field in order to analyze the segregation patterns. Plants evidencing lesion spotted leaves were counted. The best-fitted data were analyzed via Chi-square ($\chi^2$) tests.

### Phenotypes

Spot formation time and structures on the leaves at different developmental stages were investigated. Pictures of leaves from 60 day-old plants were obtained using a digital camera. Agronomic traits including days to heading (DH), tiller number (TN), culm length (CL), plant height (PH), leaf length (LL), panicle exertion ability (PE), panicle length (PL), panicle number (PN), panicle thresh ability (PT), spikelet number (SN), spikelet fertility (SF), and 100 grains weight were evaluated in *bl2* mutant rice as well as wild-type (Milliang 23) plants. The Tiller number per plant was scored as the number of reproductive tillers for each plant and the average including standard error (SE) was calculated from the data obtained from 15 plants. Spikelet fertility percentage was scored as the number of grains per panicle divided by the number of spikelets per panicle. The day on which the first developing panicle emerged approximately 1 cm beyond the leaf sheath of the flag leaf was recorded as the heading date for each plant of each accession. Days to heading (DH) values were converted from the day of transplantation to the mean heading date. One hundred ripped spikelets were dehulled and measured for gram weight. Phenotypic effects were also noted upon temperature and light treatments. A few plants were grown in the low (15°C), normal (30°C) and high (45°C) temperature conditions for 30 days in the growth chamber and then were cultivated further under normal environmental conditions. The phenotypic effect was observed at mature stage.

### Leaf anatomy

Light microscopic study was conducted using wild-type, non-spotted, and spotted flag leaves of the *bl2* mutant from 60 day-old plants. Transverse sections were visualized under an Olympus BX51 dissecting fluorescent microscope (Olympus, Japan). Observations were made under bright light, and then subsequently under UV using a 365 nm excitation filter and a 488 nm long pass emission filter. Images were captured with an Olympus C-7070 digital camera (Olympus).

For transmission electron microscopy (TEM) analysis, leaf segments (1 mm × 5 mm) were cut from the 60 day-old flag leaves of non-spotted and spotted parts of *bl2* mutant and wild-type plants. The samples were then fixed with 2.5% (v/v) glutaraldehyde in 0.1 M sodium phosphate buffer (pH 7.0) and incubated at 4°C with five buffer changes at 30 min intervals, and then transferred and maintained for 12 h at 4°C. After fixation, the samples were washed with 0.1 M sodium phosphate buffer, at neutral pH, over three 20-minute incubations at 4°C. After washing, the samples were post-fixed for 6 h in 1% (v/v) osmium tetroxide in sodium phosphate buffer (pH 7.0). Then, after three buffer washes, the samples were dehydrated through a graded ethanol series. After 15 min of incubation in propylene oxide, they were incubated further in epoxy resin solution [0.46 M EMBED-818, 0.28 M nadic methyl anhydride, 0.25 M dodecenyl succinic anhydride, 17.2 mM 2,4,6-Tri (Dimethylaminoethyl) phenol in propylene oxide at 1:1 (v/v) volume] for 4 h at room temperature. The samples were subsequently incubated in a 2:1 v/v epoxy resin solution for 12 h at room temperature, and then embedded in fresh epoxy resin solution and polymerized overnight at 70°C. Ultrathin sections were prepared with an MT-X ultramicrotome (RMC, USA). Sections were viewed using an H-7600 transmission electron microscope (Hitachi Ltd., Japan) operated at 80 kV at the microscopic analysis center at the Center for Facility at Yeungnam University, Gyeongsan, Korea. Three biological replicates were used for all microscopic analyses.

### Chlorophyll content measurement

Leaf samples were collected from 15, 30, 45, and 60 day-old plants of *bl2, spl6,* and wild-type rice for measurements of chlorophyll content. Fresh and fully expanded 20 mg leaf tissues were extracted overnight with 1 ml of 95% ethanol at 60°C. The extracts were measured at wavelengths of 645 and 663 nm with an Optizen2120 UV Spectrophotometer (Mecasys Co. Ltd., Korea). Chlorophyll *a*, chlorophyll *b,* and total chlorophyll contents were calculated using MacKinney's (1941) specific absorption coefficients, as previously described by Chory et al. (1989). The total chlorophyll per gram tissue was converted via the following formula: chlorophyll (mg/g) = chlorophyll (mg/L) × 0.001 (L) / fresh weight (g). Three biological replicates were used for this experiment.

**Enzyme extraction and catalase activity Assay**

One gram of leaf tissue from 15, 30, 45, and 60 day-old plants were ground in liquid nitrogen using a chilled pestle and mortar, and subsequently homogenized in 4.0 ml of chilled 50 mM potassium phosphate buffer (pH 7.0) containing 1.0% (w/v) insoluble polyvinylpolypyrrolidone and 1.0 mM phenylmethylsulfonylfluoride, 1.0 mM EDTA, 1.0 mM dithiothreitol (DTT), and 0.2% (v/v) Triton X-100. The homogenates were filtered through 2-fold muslin cloth and centrifuged for 10 min at 10,000 × *g* at 4°C. The supernatants were stored at 4°C and used for catalase assays within 4 h. The total protein content of the enzyme extracts was determined in accordance with the Bradford method (1976). Catalase (EC 1.11.1.6) activity was measured in a reaction mixture containing 500 μmoles $H_2O_2$ in 10 mL of 100 mM phosphate buffer (pH 7.0) and one ml of tissue extract. Decomposed $H_2O_2$ was assayed after a 5 min reaction by reading the spectrometric absorbance at 240 nm of both blanks and samples (Aebi et al., 1983; modified after Bisht et al., 1989). Corresponding blanks were maintained via the addition of 1 ml of 2 N $H_2SO_4$ prior to the addition of enzyme extract. Catalase activity is expressed as units (μmol $H_2O_2$ decomposed $min^{-1}$) $mg^{-1}$ protein. Three independent samples were assayed and standard errors among them were considered in the final results.

**Total protein content measurement**

To determine the total leaf protein content, leaf extraction was conducted according to the method previously described by Ali (2005). In brief, leaves were homogenized in 80% acetone and the pellets were dissolved overnight in 1 N NaOH. The supernatant was boiled at 90°C for 30 min and centrifuged prior to use for protein determination. Bovine serum albumin was used as a standard. Protein content was calculated against a standard curve. The results were expressed in mg protein/g leaf tissue with standard error within three biological samples.

**$H_2O_2$ level measurement**

$H_2O_2$ concentrations in the lesion-bearing leaves and normal leaves were determined via the method of Brennan and Frenkel (1977). One gram of fresh leaves from 15, 30, 45 and 60 day-old plants were homogenized in 5 ml of cold acetone and centrifuged for 10 min at 10,000 × *g*. One ml of the supernatant was mixed with 0.1 ml of 20% titanic tetrachloride in concentrated HCl (v/v) and 0.2 ml of concentrated $NH_4OH$. The reaction mixture was then centrifuged for 10 min at 10,000 × *g*, the supernatants were discarded and the pellets were dissolved in 0.75 ml of 2N $H_2SO_4$. Absorbance was measured at 415 nm against a water blank. The $H_2O_2$ concentration was calculated via comparisons of absorbency against a standard curve representing the titanium-$H_2O_2$ complex from 0.1 to 1 mM. The results were expressed in μg $H_2O_2$/mg leaf tissue with standard error within three independent experiments.

**Ascorbic acid measurement**

The ascorbic acid concentrations were determined via the ascorbate oxidase method, according to the methods developed by Tokunaga and Esaka (2007). In brief, the leaf samples were ground in liquid nitrogen and suspended in 6.0% (v/v) perchloric acid, followed by 10 min of centrifugation at 14,000 rpm at 4°C. The supernatant was appropriately diluted and 50 μl of the sample was added to 445 μl of 200 mM succinate buffer (pH 12.7, adjusted with KOH) in a spectrophotometer. The absorbance of the solution was recorded immediately and then again 5 min after the addition of 2.5 U of ascorbate oxidase at 265 nm. The ascorbic acid content was calculated via comparison with the standard curve.

**Reverse-transcription PCR for cDNA cloning**

Reverse-transcription PCR was conducted according to the methods of Kang et al. (2004). First-strand cDNA was synthesized using the Universal Riboclone® cDNA Synthesis kit (Promega, USA), according to the manufacturer's instructions. Several full length cDNAs including protein disulfide isomerase (*OsPDI*, accession: AY987391), thyrodoxin peroxidase (*OsTPX*, accession: AM039889), glutathione peroxidase (*OsGPX1*, accession: AY100689) and rice actin (*OsActin1*, accession: NM_001062196) were PCR amplified. *Taq* DNA polymerase (Promega) was used for PCR using the following thermal cycles: denaturing at 95°C for 2 min, followed by 29 cycles of denaturing at 95°C for 1 min, annealing at 55°C for 2 min and extension at 72°C for 2 min, and one cycle of extension at 72°C for 5 min. Gene-specific primers were as follows, *OsPDI*-183F, 5′-CGT CGA GTT CTA CGC CCC GTG-3′; *OsPDI*-987R, 5′-CAG CCC AAA GTA CTG GAA GGC-3′, *OsTPX*-1F, 5′-ATG GCC GCC TGC TGC TCC TCC-3′; *OsTPX*-786R, 5′-TTA GAT GGC CGC GAA GTA CTC-3', *OsGPX1*-F, 5′- AAC GAA TTC CCG CCG CGC CGT CCG C-3′; *OsGPX1*-R, 5′- TTC TCG AGA GAG CTC CCA AGC AG-3′; and *Osactin1*-1F, 5′- ATG GCT GAC GAG GAT ATT CAA-3′; *Osactin1*-1310R, 5′-TCA GAA GCA CTT CAT ATG GAC-3′. PCR products were cloned into pGEM-T Easy vector (Pro-mega). Nucleotide sequencing was conducted via the Bigdye termination method using ABI 3700 DNA analyzer (Applied Biosystem, Hitachi, Ltd.) at the Institute of Biotechnology, Yeungnam University, Gyeongsang, Korea. The cloned PCR products were then isolated and purified from the plasmid for use as probes.

**Northern blot analysis**

Northern blot analysis was conducted in accordance with the methods developed by Kang et al. (2004). In brief, 20 μg of total RNA was electrophoretically separated on 1.4% denaturing agarose gel using 1× MOPS [3-(N-morpholino)-propanesulfonic acid] buffer, then transferred to Nytran® nylon membranes (Schleicher & Schuell Bioscience, USA) with 25 mM sodium phosphate buffer (pH 7.0) for 12 h. The membranes were exposed to UV at 1200J. Radioactive-labeled probes were generated from the RT-PCR cloned *OsPDI*, *OsTPX*, *OsGPX1* and *Osactin1* genes using a random labeling system (Promega). Prehybridization was conducted at 42°C for 3 h in 50% (v/v) formamide, 6× SSC (1× SSC is 0.15 M NaCl, 0.25 M $NaH_2PO_4$ and 25 mM $Na_2EDTA$), 5× Denhardt's solution [1% (w/v) Ficoll, 1% (w/v) polyvinylpyrrolidone, 1% (w/v) bovine serum albumin], 0.5% (w/v) SDS, and 0.1 mg/ml Herring sperm DNA. Hybridization was conducted for 14 h using α-[$^{32}$P] dCTP labeled probes at 42°C. The membranes were then washed twice in 2× SSC and 0.1% SDS solution at room temperature for 5 min, followed by washing in 1× SSC and 0.1% SDS solution at room temperature for 10 min, in 0.1× SSC and 0.1% SDS solution at room temperature for 20 min and in 0.1× SSC and 0.1% SDS solution at 42°C for 5 min. For autoradiography, the membranes were exposed to X-ray film (Fuji Photo Film Co., Japan) for 24 h.

## RESULTS

**The *bl2* mutant phenotype was unique in LMMs**

A *bl2* mutant germplasm evidenced a phenotype characterized by dark reddish-brown spots of various sizes on the leaf surface. As is shown in Fig. 1, spots were spread over the entire leaf surface with advanced aging. The irregular lesions were

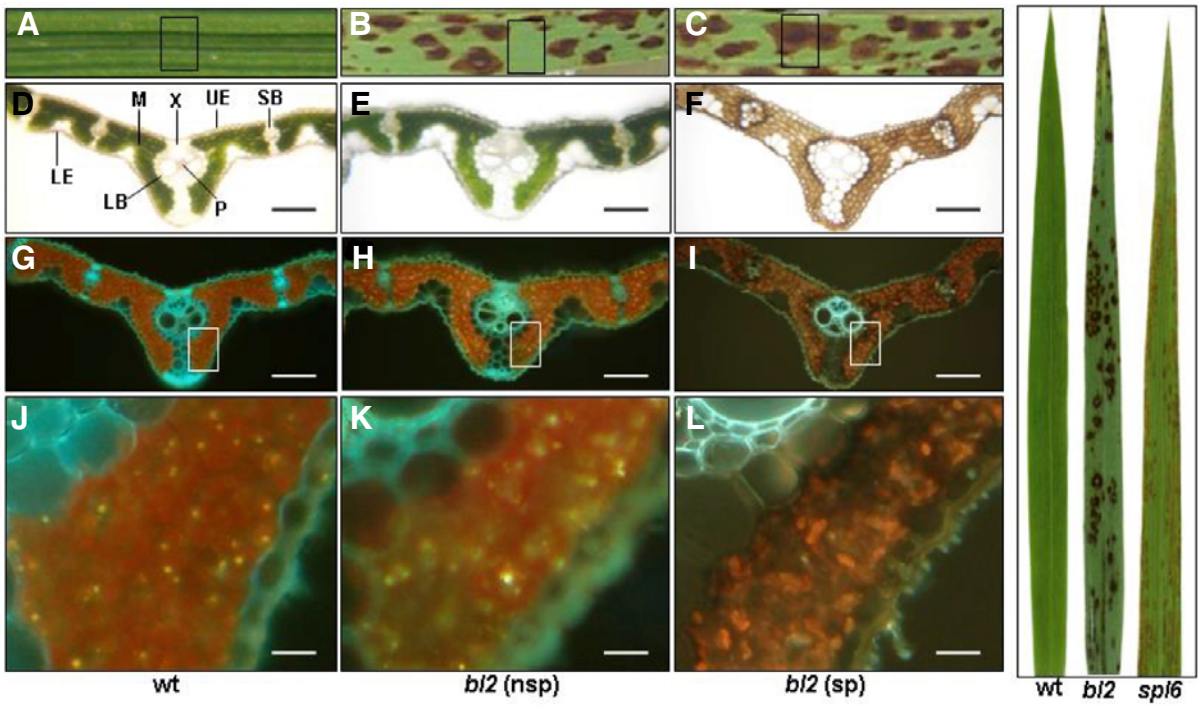


**Fig. 1.** Light microscopy analysis of spotted and non-spotted leaf blades of the *bl2* mutant and the wild-type rice. (A-C) Parts of the fully expanded 90-day old fresh leaves of the wild-type and *bl2* mutant. (D-F) Transverse sections of the boxed parts of A, B and C, respectively, observed under white light and (G-I) observed under UV light at 488 nm. (J-L) Magnified view of boxed area of G, H, and I, respectively. A, D, G and J are wild-type (wt) leaf sections. B, E, H and K are non-spotted (nsp) and C, F, I, and L are spotted (sp) leaf sections of the mutant. Indications in D are LB, large vascular bundle; LE, lower epidermis; M, mesophyll cell; P, phloem; SB, small vascular bundle; UE, upper epidermis and X, xyleme. Bars indicate 100 μm in D-I and 25 μm in J-L. Full leaves of the wild type, *bl2* and *spl6* mutants are represented in the right box.

visible as early as the four-leaf stage, which was unique among our previously studied lesion mimic mutants (Kang et al., 2007; Matin et al., 2010). At the seedling stage, a few small brownish spots appeared over the leaf surface, which became larger and more visible at the tillering stage and spanned the entirety of the leaf surface. Interestingly, lesions also formed on the leaf sheaths of the *bl2* mutant. Spots were noted at all developmental stages and formations of new spots were observed with plant maturity, and thus the lesions covered the leaf blades at flowering time. Although the majority of the spots were small in the tillering stage, they became much larger with maturity (Fig. 1). At maturity, almost all of the leaves were affected by the spots. Owing to the profound severity of spot formation at the maturation stage, senescence occurred earlier than in the wild-type plants. The lesions developed from older to younger leaves throughout the stages of plant development.

Environmental factors including light and temperature affected the phenotypic severity of the mutant plants. Mutant plants were grown in the growth chamber with high-intensity light for 10 days and under high temperatures (45°C for 30 days). The treated plants produced increased numbers and larger-sized spots on the leaves relative to the plants grown under normal environmental conditions. Moreover, the chlorotic sectors became more extensive in the treated plants. However, plants grown under 10 days of continuous dark conditions and leaf areas covered by aluminum foil before spot formation evidenced less severe spot coverage than was observed in the plants grown under normal conditions (data not shown). This may be attributable to the profound photo-oxidative damage observed under higher light intensity and temperature.

**Leaf anatomical features of the *bl2* were similar to those of *spl6***

To characterize the differences in the mesophyll chloroplasts of the wild-type and *bl2* leaves, microscopic analysis was conducted as described by Kang et al. (2007). The anatomical features of the flag leaves of the wild-type (Fig. 1A) and *bl2* plants (Figs. 1B and 1C) were observed under fluorescent light with and without UV emission, using a light microscope. In the wild-type leaf section, as well as the non-spotted part of the *bl2* leaf, the mesophyll cells were green, indicating that they were filled with chloroplasts (Figs. 1D and 1E). In the spotted parts, however, the mesophyll cells were dark brown, with very few greenish parts (Fig. 1F), indicating the absence of chloroplasts and the death of the mesophyll cells. The clear differences in color reflection noted among the leaf sections were noted under UV light at 488 nm. The mesophyll cells of the wild-type and non-spotted parts of the mutant leaves were reddish (Figs. 1G and 1H), implying the reflection of non-absorbed light by the chloroplasts. Conversely, the mesophyll cells of the spotted area did not turn red, thus reflecting the degradation of the chloroplasts in the mesophyll cells (Fig. 1I). This indicates that those cells were dead. Transmission electron microscopy (TEM) analysis of the wild-type and non-spotted and spotted leaf sections of the mutant indicated a clear cellular difference among the samples. In the wild-type section, the mesophyll chloroplasts were phenotypically normal with a typical lens shape, chloroplast wall, well-developed thylakoid and granal

**Table 1.** Phenotypes of wild type cultivar (YUC013, Milliang23) and two *bl2* mutant germplasms (YUM013 and YUM057) grown under natural field conditions

| ID | DH ± SE | CL ± SE | LL ± SE | LW ± SE | PH ± SE | TN ± SE | PE | PL ± SE | PN ± SE | PT | SN ± SE | SF ± SE | GW ± SE |
|---|---|---|---|---|---|---|---|---|---|---|---|---|---|
| YUC 013 | 73 ± 1.3 | 61.5 ± 1.2 | 50.9 ± 0.9 | 1.7 ± 0.1 | 111.5 ± 5.2 | 23 ± 1.0 | 1 | 22.5 ± 0.6 | 21 ± 1.0 | 1 | 130 ± 3.4 | 92.5 ± 0.5 | 2.5 ± 0.1 |
| YUM013 | 65 ± 1.1** | 55.5 ± 0.6** | 54.5 ± 0.6** | 1.6 ± 0.1 | 108.6 ± 3.8 | 11 ± 1.4** | 1 | 24.1 ± 0.5* | 10 ± 1.4** | 1 | 70.6 ± 2.4** | 66.7 ± 1.4** | 2.2 ± 0.1* |
| YUM057 | 76 ± 1.4** | 45.3 ± 0.4** | 45.4 ± 0.7** | 2.0 ± 0.2* | 90.5 ± 7.2** | 6 ± 1.1** | 2 | 22.0 ± 0.8 | 04 ± 1.1** | 2 | 53.4 ± 7.3** | 49.3 ± 2.3** | 2.0 ± 0.1** |

ID, identity of the wild type cultivar (YUC013, Milliang23) and independent two mutant lines (YUM013 and YUM057) that showed similar phenotypes; DH, days to heading (defined as duration from transplantation to emergence of the first panicle); CL, culm length in centimeter (cm); LL, leaf length in cm; LW, leaf width in cm; PH, plant height; TN, number of reproductive tiller per plant; PE, panicle exsertion ability (Scale: 1; well exserted, 2; moderately well exserted); PL, panicle length in cm; PN, panicle number per plant; PT, panicle thresh ability [Firmly grasp and pull the hand over the panicle and estimate the percentage of shattered grains, scale: 1, difficult (less than 1%); 2, intermediate (6-15%)]. SN, spikelet number per panicle; SF, spikelet fertility percentage per plant; GW, 100 grains weight in gram; SE, standard error of five observation for each trait. *, ** indicate that phenotypes between wild type and mutants were significantly different (*t*-test, P < 0.05, 0.01 respectively).

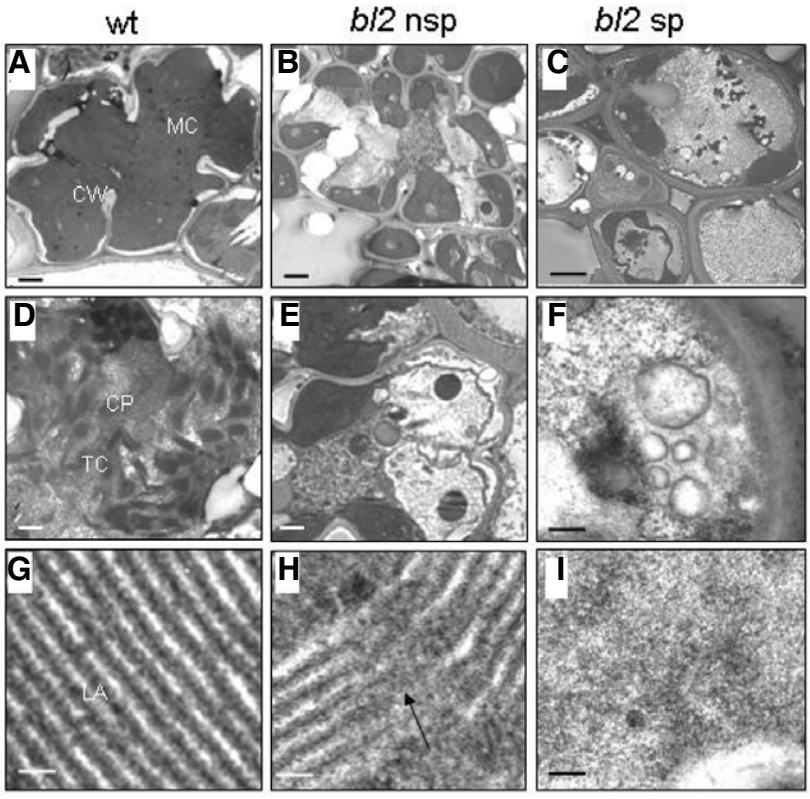


**Fig. 2.** Transmission electron microscopy (TEM) analysis of the wild-type and *bl2* leaves. (A-C) TEM of the ultrastructure of chloroplasts of wild-type and non-spotted (nsp), and spotted (sp) leaf blades of *bl2* mutant, respectively. (D-F) Close-ups of one chloroplast of wild type, nsp and sp leaves, respectively. (G, H) Close-ups of thylakoids with lamella of wild type and nsp of mutant leaf sections. (I) Close-up of cell inside of sp section of the mutant. Indications in the figures are CP, chloroplast; CW, chloroplast wall; LA, lamella; MC, mesophyll chloroplast; TC, thylakoids, and ST, stroma. Arrow heads in the H indicate broken lamella. Developed and matured flag leaves of the plants were used. Bars: A-C; 0.5 μm, D; 0.5 μm, E; 2 μm, F; 0.1 μm, G-I; 0.1 μm.

stacking and lemma (Figs. 2A, 2D and 2G). By way of contrast, a large proportion of the chloroplasts observed in the *bl2* non-spotted leaf sections evidenced an abnormal shape with fewer and more damaged chloroplasts, as well as disorganized thylakoid membrane, and damaged or broken lamella (Figs. 2B, 2E and 2H). Whereas the mesophyll cells in the spotted leaf area were empty and evidenced broken chloroplast walls, damaged cellular organelles, shrunken cell size, and visible osmophilic and electron-dense particles such as plastoglobules were noted within the cells. (Figs. 2C, 2F and 2I).

**Agronomic characteristics of the *bl2* mutant were disgraceful**

In an effort to gain insight into the agronomic features of the *bl2* mutant, several important agronomic traits were observed in the two germplasms of the *bl2* mutant variants (YUM013 and YUM057), which were independent mutant lines identified from EMS mutagenesis, as well as in the wild-type plant (Milliang23). Apart from the spotted phenotypes, significant differences between the mutant and the wild-type plants were noted in terms of several agronomic traits including days to heading, plant stature, tillering ability, leaf structure, grain structure and quality, and panicle structure (Table 1). The mutant plants evidenced abnormal developmental phenotypes with various degrees of agronomic characteristics and significantly lower trait values than the controls (Table 1). The mutants evidenced reduced tiller and panicle numbers, 11 and 10 for YUM013, and 6 and 4 for YUM057 relative to the wild-type, 23 and 21, respectively (Table 1). Owing to the early senescence occurring due to cell death in the *bl2* variants, it evidenced a shorter lifespan than the wild-type plants grown under identical environmental conditions. Plant stature, tillering ability, panicle formation ability, and seed setting rates were lower than those of the cultivar controls.

**Table 2.** Segregation of *bl2* mutant phenotype in the $F_2$ generation

| Cross | $F_1$ phenotype | $F_2$ segregation for *bl2* gene | | | | $\chi^2$ (3:1) | *p*-value |
|---|---|---|---|---|---|---|---|
| | | Number | Wild type | Mutant | Total | | |
| *bl2*/Iilpoom | Wild type | Observed | 192 | 52 | 244 | 1.77 | 0.90-0.10 |
| | | Expected | 183 | 61 | 244 | | |
| *bl2*/M23 | Wild type | Observed | 134 | 42 | 176 | 0.12 | 0.90-0.10 |
| | | Expected | 132 | 44 | 176 | | |

Phenotype of the female parent (*bl2*) was mutant and pollen donor, Ilpoombyeo and Milliang23 (M23) was wild type. Probability of acceptance of the $\chi 2$ value is calculated using $df = 1$.

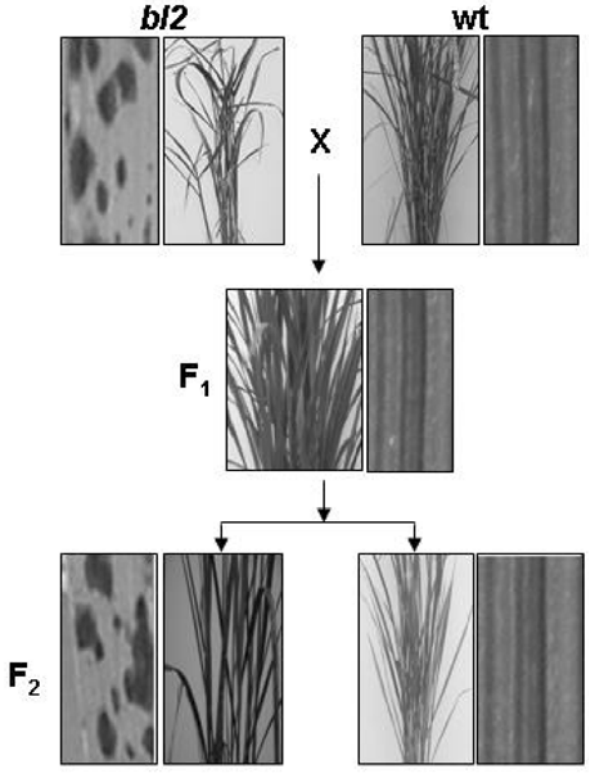


**Fig. 3.** Genetic segregation of *bl2* mutant at $F_1$ and $F_2$ progenies. Cross was made between wild type normal rice and *bl2* mutant. Whole plant and magnified leaves are indicated. $F_1$ had wild type phenotype, whereas, in the $F_2$, mutant and wild type segregation was observed.

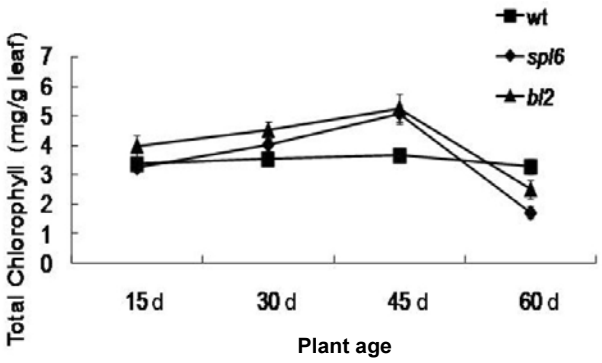


**Fig. 4.** Relative total chlorophyll content in the *spl6, bl2* and wild-type plants grown under natural environmental conditions. Fully expanded fresh leaves of 15, 30, 45 and 60 days old plants were used. Concentrations are expressed as mg/g fresh tissue. Values are average of three replicates (mean ± SE).

### The inheritance pattern of the *bl2* mutant was followed by a single recessive gene

The genetic nature of the *bl2* mutant was analyzed from the cross between the mutant and wild type *japonica* (Ilpoombyeo) and *indica* (Milliang23) cultivars used either as pollen donors or pollen receptors. The $F_1$ plants from all of the cross-combinations evidenced phenotypes similar to those of the wild-type plants (Table 2; Fig. 3). Large numbers of $F_2$ seeds were collected from each single $F_1$ plant and were further grown under natural field conditions. Among the $F_2$ segregation progenies, 52 plants evidenced a recessive spotted phenotype, whereas 192 plants evidenced the dominant wild type (non-spotted) phenotype from the cross between the mutant and Ilpoombyeo variants (Table 2; Fig. 3). The results of $\chi^2$ analysis revealed that $F_2$ progenies segregated at a 3 wild-type: 1 mutant ratio with the *bl2* gene, with a value of $\chi^2_{(3:1)} = 1.77$ (Table 2). Moreover, the $F_2$ population of the cross of *bl2* and Milliang23 also segregated at a 3: 1 (wild type: mutant) ratio with a satisfactory fit ($\chi^2_{(3:1)} = 0.12$) (Table 2). The segregation of $F_2$ populations confirmed that the mutant characteristics are governed by a single recessive gene.

### Chlorophyll content in *bl2* and *spl6* mutants were higher than that of normal rice

Total chlorophyll was measured from the leaf extraction of the wild-type, *spl6,* and *bl2* mutants to compare the chlorophyll content within the samples at 15, 30, 45 and 60 days of plant age, as well as between the wild-type and mutants. At 15 days of age, the total chlorophyll content of the samples was almost identical for all samples, whereas the total chlorophyll contents increased with further plant development until 45 days in the mutant variant (Fig. 4). In the wild-type leaves, chlorophyll contents were almost identical, with a slight reduction at day 60; however, a sizeable difference was noted between the wild-type and mutants at day 45, whereas the total chlorophyll contents were 38.79% higher in *spl6* and 48.44% higher in *bl2* relative to the wild-type leaf samples (Fig. 4). Total chlorophyll contents were almost 10% higher in the *bl2* mutant than the *spl6* mutant at day 45. The mutant evidenced a dramatic reduction in chlorophyll content by more than 2-fold at day 60 from that of day 45, whereas, an insignificant reduction was observed in the wild-type (Fig. 4).

### Hydrogen peroxide levels were elevated in the *bl2* mutant

$H_2O_2$ levels, a symptomatic indicator of cell death in plants, were measured in the wild-type and mutant leaves. The $H_2O_2$ levels also followed the same trend as that of the chlorophyll

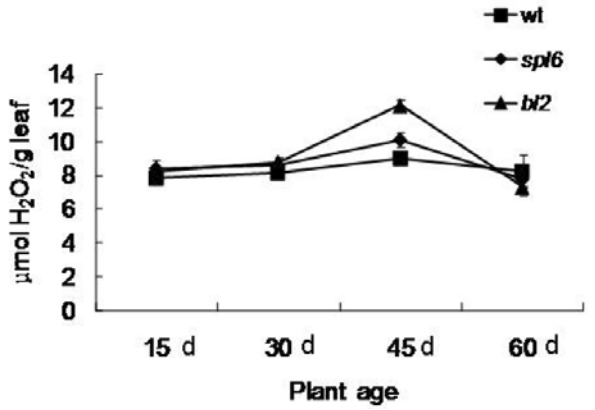


**Fig. 5.** Relative $H_2O_2$ concentrations in wild-type, *spl6* and *bl2* mutants occurring in the plants grown under natural conditions. Samples were used from 15, 30, 45, and 60 days old plants. Concentrations are expressed as μmol/g fresh leaf tissue. Each value is the mean of three individual replicates (mean ± SE).


**Fig. 6.** Total protein content in wild type, *spl6* and *bl2* leaves at 15, 30, 45 and 60 day old rice plants. Protein contents are expressed as mg/g fresh leaf tissue. Total protein content was reduced with growth period in the wild-type, *spl6,* and *bl2* leaves. No significant differences were detected between the wild-type, *spl6,* and *bl2* leaves.

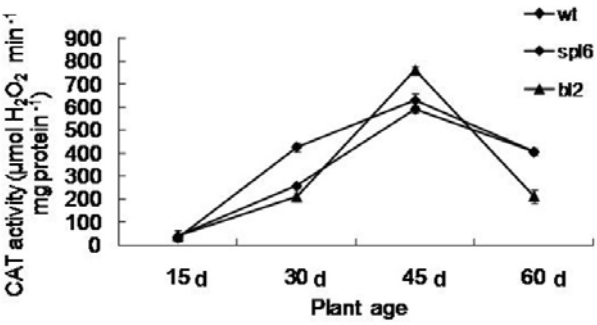


**Fig. 7.** Catalase activity in the wild-type, *spl6,* and *bl2* leaves at 15, 30, 45 and 60 days of growth. Activity was expressed as μmol $H_2O_2$ decomposition per min per mg protein. Activity was increased until 45 days of growth after germination and reduced activity was noted at day 60 after germination.

contents in the wild-type, *spl6,* and *bl2* mutant leaves (Fig. 5). Initially, at day 15, similar levels of $H_2O_2$ were observed among the leaf samples. Thereafter, the level of hydrogen peroxide increased differentially and reached a maximum at day 45, which was 12.21% higher in the *spl6* variant and 34.63% higher in the *bl2* variant than in the wild-type. However, these levels were reduced dramatically at day 60 in the mutants (Fig. 5). Higher levels of $H_2O_2$ in *bl2* leaves relative to the wild-type and *spl6* variants were closely related with unique spot formation pattern in the mutant.

**Total protein content did not differ significantly among *bl2*, *spl6,* and wild-type**

To evaluate the relative levels of total proteins in the wild-type and mutant leaves, the total protein contents were spectrophotometrically measured at differential developmental stages of the plant age. We noted no significant differences in total protein content among the wild-type, *spl6,* and *bl2* leaves (Fig. 6). However, slight reductions with growth period and lower contents were detected at 45 days and then increased slightly at 60 days of plant age (Fig. 6).

**Catalase activity increased in the mutant**

Catalase activity was measured in the mutant and wild-type leaves at different developmental stages. The lowest level of activity was found at 15 days of age in all samples (Fig. 7). Thereafter, the catalase activity gradually increased up to 45 days of plant age and declined later on, regardless of the samples. In the case of *bl2*, the elevation level of catalase activity was highest at 45 days among all samples, whereas a drastic reduction was apparent at 60 days (Fig. 7). The activity was 20.03% higher at 45 days than the other growth stage in the *bl2* leaves, whereas it was almost identical in the wild-type and *spl6* leaves (Fig. 7).

**Total ascorbic acid contents evidenced a gradual increment during growth period in the mutants**

Ascorbic acid contents were measured in the leaves at various developmental stages of the mutants and wild-type plants. Increasing similar levels of ascorbic acid contents were noted among samples from 15 days to 45 days of age, and differed significantly at 60 days of age (Fig. 8). In the wild-type leaves, ascorbic acid contents were reduced slightly at day 60 relative to the 45 day-old leaf samples, even though these levels were higher than measured in the 15 day-old leaf samples. Until 60 days of age, ascorbic acid contents increased in the *spl6* leaves, whereas the levels of ascorbic acid increased slightly in the *bl2* leaves (Fig. 8). Almost two-fold higher contents of ascorbic acid were noted in the *bl2* leaves, whereas the levels were almost three-fold as high in the *spl6* leaves relative to the wild-type at 60 days of age (Fig. 8). Specifically, the ascorbic acid contents of the s*pl6* mutant plants were almost one and-a-half fold that of the *bl2* variant at 60 days.

**Some stress response genes were expressed indelibly in the *bl2* mutant**

Phenotypic expression in the *bl2* mutant is affected by stress conditions. Therefore, we evaluated the expression of the metabolism and stress-associated genes *OsPDI, OsTPX* and *OsGPX1* via Northern blot analysis. Northern blotting was conducted using total RNA isolated from the wild-type and non-spotted and spotted leaves of the mutant. Owing to severe spot formation during the maturation stage, the *bl2* mutant leaves become chlorotic and exhibit early senescence. Therefore, we evaluated the expression of genes associated with stress response in the mutant leaves before lesions development and after severe lesion formation. The expression of the *OsActin1* gene was also analyzed as an experimental control. The ex-

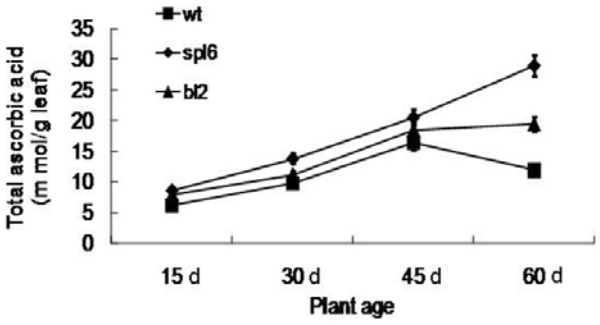


**Fig. 8.** Total ascorbic acid contents in wild-type, *spl6,* and *bl2* leaves at 15, 30, 45 and 60 day-old plants. Ascorbic acid content was expressed as mmol/g fresh leaf tissue.

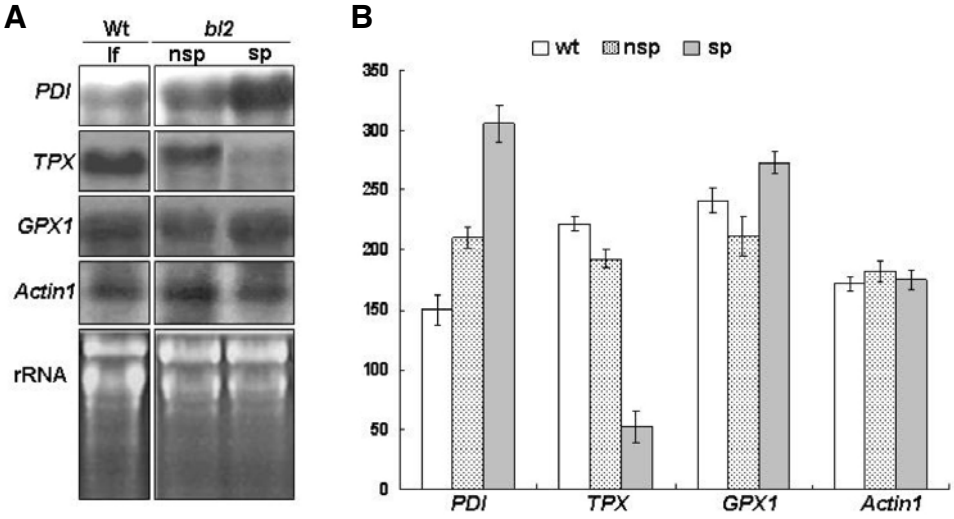


**Fig. 9.** Gene expression analysis in *bl2* mutant and wild-type rice. (A) Expression of *OsPDI*, *OsTPX*, *OsGPX1* and *Actin1* at the RNA level of wild-type and *bl2* mutant. *Actin* was used as experimental control. Total RNAs were extracted from leaves (lf) of wild-type rice as well as matured spotted (sp) and non-spotted (nsp) leaves of the *bl2* mutant. Twenty micrograms of total RNAs were loaded in each lane. Ribosomal RNA bands are shown as loading control for each RNA blot. Two independent experiments were conducted. (B) Relative expression intensity of the gene transcription in wild-type (wt), and non-spotted (nsp) and spotted (sp) leaves of the *bl2* mutant. Values are the means ± SE of transcription levels of the genes. Results are from two independent Northern blot experiments of the same biological samples.

pression of the *OsPDI* transcript was significantly increased in the spotted leaves relative to the non-spotted leaves, whereas, the increment in the spotted leaves was more than 2-fold that of the wild-type controls (Fig. 9). The expression of *OsTPX* occurred in a precisely opposite fashion, in that expression was reduced slightly in the non-spotted leaves than the wild-type, whereas, the reduction in the spotted leaves was more than 4-fold that of the non-spotted as well as wild-type leaves (Fig. 9). *OsGPX1* expression did not induce significant changes regardless of samples; however, expression was increased slightly in the spotted leaves relative to the non-spotted leaves. The expression of *OsActin1*, which was used as an experimental control, was similar for all samples. The EtBr-stained RNA gels predicted the non-degradation of total RNAs of the wild-type and *bl2* non-spotted and spotted leaves, respectively (Fig. 9).

## DISCUSSION

In order to gain further insight into the basis of phenotypic expression in the *bl2* mutant and to compare it with the rice *spl6* lesion mimic mutant, we have evaluated the physiological, morphological and anatomical phenotypes of the mutants at various stages of development. We also evaluated the relationships between total chlorophyll, hydrogen peroxides, ascorbic acid, and total protein content and catalase activity with the plant developmental stages corresponding to spot initiation and severe lesion formation. The uniqueness of the spot structure and formation pattern of the *bl2* mutant reflected its differences from many other identified rice lesion mimic mutants. Among the several rice *lrd* families characterized thus far, the brown leaf spot 2 (*bl2*) mutant included the brown leaf spot family (Kinoshita, 1995; Singh et al., 1995). Tinny spots became visible at approximately 30 days of age in the seedlings and gradually became larger and assumed a dark brown color. Several *lrd* mutants have been identified in rice thus far, including *spl11*--which evidences a spontaneous cell death phenotype on the leaves (Yin et al., 2000), *Spl7*--which involves relatively small and reddish-brown lesions scattered over the whole surface of leaves (Yamanouchi et al., 2002), *spl1*--which involves spontaneous disease-like lesions in the absence of pathogen (Liu et al., 2004), *spl6--which* involves spontaneous necrotic lesions at the late tillering stage (Kang et al., 2007), and *SPL28*--which is responsible for spotted leaves and early senescence (Qiao et al., 2010). All of those mutants have been extensively studied and specific genes were found to be associated with phenotypic formation in the mutants, including heat stress transcription factor, U-box, and armadillo repeat protein, as well as the clathrin-associated adaptor protein (Qiao et al., 2010; Yamanouchi et al., 2002; Yin et al., 2000). However, the *bl2* mutant, which evidences individual phenotypic characteristics, has not yet been assessed in terms of its molecular functions.

Many important agronomic characteristics of rice-- including yield, plant height, and flowering time--have been described, and shown to be controlled by a number of quantitative trait loci (QTL). Several genes have been implicated in the control of

days-to-heading, plant height, and number of grains per panicle (Wei et al., 2010). In the *bl2* mutant, we have discussed several important agronomic characteristics and compared them with those of the mutant phenotype. In the mutants, some important agronomic traits differed from those of the wild-type plants. Thus, it is anticipated that the *bl2* mutant gene might be associated with aspects of plant physiology and morphology. These findings may prove useful in the identification of gene functions and in exploring mechanisms in the mutant phenotype related to flowering time and day length, as well as heading time. The inheritance pattern of the *bl2* mutant was assessed in a cross between a pollen receptor with the LMM mutant phenotype *bl2* and a normal wild-type rice pollen donor. $F_1$ phenotypes and segregation phenotype of $F_2$ progenies revealed that the *bl2* mutant was recessive. Several lesion mimic mutants (LMM) have also been studied in different crops. Most rice lesion mimic mutants have been characterized as recessive (Matin et al., 2010; Nagato and Yoshimura, 1998; Sing et al., 1995). However, the majority of the lesion mimic mutants studied in maize were found to be dominant (Johal et al., 1995).

During cell death or leaf senescence, the chloroplast is one of the earliest targeted cellular organelles to be broken down. Therefore, we have evaluated the relationship between chlorophyll content and the stage of spot severity. Total chlorophyll content was increased during severe spot formation, and then drastically reduced. This led us to predict that cell death occurs as the result of an oxidative burst resulting from higher photosynthesis, which might be explained by the higher total chlorophyll contents in the mutant leaves. A significant correlation was determined to exist between the chlorophyll contents and the rate of photosynthesis (Hu et al., 2009). A positive correlation was found to exist between the chlorophyll content and plant age, and during senescence, it was reduced slightly in the rice plant (Wang et al., 2008). The drastic reduction observed at the later stage might have resulted from the degradation of chloroplasts in the mutants due to severe cell death and early senescence. Moreover, we evaluated chlorophyll degradation from the leaf anatomy of the mutants (Figs. 1 and 2).

The formation of lesions in *spl6* and *bl2* leaves was associated with developmental stage. Chlorophyll content was obviously increased in leaves at 45 days of age, resulting in higher rates of photosynthesis; additionally, elevated oxidative toxicity might result in cell death and expose the leaf surface to severe lesion formation. With regard to the most important agronomic traits, *bl2* evidenced lower trait values relative to the wild-type controls. This observation was similar to that reported for *spl6* (Matin et al., 2006; 2010). Lower quality in LMM rice and rice resistance against rice fungal blast and bacterial blight were commonly observed (Mizobuchi et al., 2002; Wu et al., 2008; Yin et al., 2000). Therefore, damage to photosynthetic leaves might be a principal cause of lower quality in the mutants. However, our observations verified that damage to chloroplasts is the principal reason for cell death and spot formation in mutant leaves. The intracellular pattern observed via TEM also showed less significant differences between spot formation in the *bl2* and *spl6* variants. In both cases, the exposure to spots owing to damage to the cellular organelles resulted in cell death.

Plant responses to environmental stress have been associated with activated forms of oxygen, including $H_2O_2$, singlet oxygen, superoxide, and the hydroxyl radical. The uncontrolled production of reactive oxygen can inactivate biomolecules or initiate chain reactions that destroy membrane structure and function. $H_2O_2$ would be endogenously generated by the metabolic pathway, and excess $H_2O_2$ production is indicative of PCD in plant cells (Brodersen et al., 2002). Therefore, we assessed $H_2O_2$ concentrations in the mutant cells. High levels of $H_2O_2$ accumulation were noted in the rice with increasing numbers of lesions in the *OsSRT1* downregulated plants (Huang et al., 2007). In this study, the highest levels of $H_2O_2$ accumulation in the mutant leaves were detected when severe cell death began at 45 days of plant age (Fig. 5), which might indicate that toxic levels of $H_2O_2$ cause plants to kill their own cells. Thereafter, reductions in the later stage (Fig. 5) may be attributable to the activation of scavenging enzymes, as well as complete cell death. Many cellular compounds function as scavengers, thereby detoxifying ROS. Enzymatic defenses include superoxide dismutases which convert the superoxide radical to $H_2O_2$, and the catalases and peroxidases which trigger the conversion of $H_2O_2$ to water and oxygen under normal conditions, which are adequate to handle the oxidative load (Walker and McKersie, 1993). Lower levels of catalase activity can impair the plant's ability to detoxify the product of oxygen photoreduction (Baker, 1994). It is generally assumed that an increase in catalase activity results in a simultaneous reduction in $H_2O_2$ contents. If catalase is the preliminary detoxifier of hydrogen peroxide, then there should be a correlation between higher CAT activity and lower $H_2O_2$ concentrations. Presumably, when lesion development was accelerated in the *spl6* and *bl2* mutants, thereby resulting in higher ROS accumulation, then CAT was also upregulated, thereby scavenging ROS in the damaged cells, and thus lowering the levels of $H_2O_2$. It has been previously observed that spots formed earlier in the *bl2* leaves than the *spl6* leaves and spot severity exposure was also observed in *bl2* leaves earlier than in *spl6* leaves; this may help to explain the higher $H_2O_2$ levels in *bl2* leaves, which evidenced a 22.43% higher yield than the *spl6* plants at 45 days of age.

We have analyzed the ascorbic acid quantity in the mutants and wild-type leaves (Fig. 8). Ascorbic acid is an abundant small mole-cule in plants and constitutes a key substance in the network of anti-oxidants. In plants, it has also been shown to perform multiple roles in developmental processes (Asada, 1999; Conklin, 2001; Shin et al., 2008; Smirnoff, 1996) as well as cell division and expansion (Kato and Esaka, 1999). Ascorbic acid is a signal molecule involved in defense responses in plants (Pastori et al., 2003). In wild leaves, in the present study, ascorbic acid contents were correlated with total chlorophyll content, $H_2O_2$, or catalase activity, but in the mutant leaves the ascorbic acid contents evidenced different patterns as they gradually increased upon increasing plant age corresponding to spot severity (Fig. 8). Although the evidence is not dispositive, differences in ascorbic acid contents between wild-type and mutant leaves and the correlation between increasing amounts of ascorbic acid and increasing spot quantity suggest that ascorbic acid plays a role in the detoxification of ROS generated in the mutant leaves. By way of contrast, reduced levels of ascorbic acid content were noted subsequent to wound stress in the leaves (Badejo et al., 2009), whereas ascorbic acid-associated genes were induced during wounding (Badejo et al., 2009).

Upon lesion formation in the LMM, the chloroplast is the first target to be damaged, resulting in effect on the photosynthetic machinery. Therefore, we investigated the genes associated with components of the chloroplast via Northern blot analysis. As shown in Fig. 9, *PDI* and *GPX1* transcripts were upregulated in the spotted leaves of the mutant strain. This may imply that overexpression is linked to lesion formation and cell death in the *bl2* mutant, thereby facilitating the mechanisms underlying protection against stress conditions. *PDI* was found to be multifunctional in plants. These functions may include various roles, most notably a physiological role in stress-induced cell death (Ray et al., 2003). *OsGPX1* is a stress-inducible gene that pro-

tects cells against oxidative stress and its transcription was induced under stress conditions in the rice seedlings (Kang et al., 2004). Upon the formation of hypersensitive responses, such as spontaneous lesion formation on leaves, the upregulation of defense-related marker genes was noted in the *OsACDR1* mutant rice (Kim et al., 2009). However, the *TPX* transcript levels were severely reduced in all the spotted leaves relative to the non-spotted and wild-type leaves (Fig. 9). Even though *TPX* is a ROS scavenger which reduces hydrogen peroxide ($H_2O_2$) via the intracellular redox signaling pathway (Hiraga et al., 2001; Schröder et al., 1998), the reduced transcript in the *bl2* mutant leaves might be not directly associated with this. Moreover, the internal experimental control, the actin, was equally expressed regardless of the sample assessed (Fig. 9).

This study provides basic information regarding the *bl2* type LMM mutant. The genetic definition of the *bl2* gene will be documented further in the future. Additionally, further research is expected to contribute to the cloning and identification of the gene, as well as to our knowledge of gene functions and the mechanisms underlying phenotypic expression.

## ACKNOWLEDGMENT

This research was supported by the National Research Foundation of Korea, Grant 521-2007-1-F0003.

## REFERENCES

Aebi, H.E. (1983). Catalase. In: Methods of Enzymatic Analysis. H.U. Bergmeyer, ed., (Weinhim, Germany: Verlag), pp. 273-286.

Ali, M.B., Hahn, E.J., and Paek, K.Y. (2005). Effects of light intensities on antioxidant enzymes and malondialdehyde content during short-term acclimatization on micropropagated *Phalaenopsis* plantlet. Environ. Exp. Bot. *54*, 109-120.

Asada, K. (1999). The water-water cycle in chloroplasts: scavenging of active oxygen and dissipation of excess photons. Annu. Rev. Plant Physiol. Plant Mol. Biol. *50*, 601-639.

Badejo, A.A., Fujikawa, Y., and Esaka, M. (2009). Gene expression of ascorbic acid biosynthesis related enzymes of the Smirnoff-Wheeler pathway in acerola (*Malpighia glabra*). J. Plant Physiol. *166*, 652-660.

Baker, N.R. (1994). Chilling stress and photo synthesis. In: Causes of photo oxidative stress and amelioration of defense systems in plants. C.H. Foyer, and P.M. Mullineaux, eds., (Boca Raton, FL: USA, CRC Press), pp. 127-154.

Balague, C., Lin, B., Alcon, C., Flottes, G., Malmstrom, S., Köhler, C., Neuhaus, G., Pelletier, G., Gaymard, F., and Roby, D. (2003). HLM1, an essential signaling component in the hypersensitive response, is a member of the cyclic nucleotide-gated channel ion channel family. Plant Cell *15*, 365-79.

Bisht, S.S., Sharma, A., and Chaturvedi, K. (1989). Certain metabolic lesions of chromium toxicity in radish. Indian J. Agric. Biochem. *2*, 109-115.

Bouchez, O., Huard, C., Lorrain, S., Roby, D., and Balagué, C. (2007). Ethylene is one of the key elements for cell death and defense response control in the Arabidopsis lesion mimic mutant *vad*. Plant Physiol. *145*, 465-477.

Bradford, M.M. (1976). A rapid and sensitive method for the quantitation of microgram quantities of protein utilizing the principle of protein-dye binding. Anal. Biochem. *72*, 248-254.

Brennan, T., and Frenkel, C. (1977). Involvement of hydrogen peroxide in the regulation of senescence in pear. Plant Physiol. *59*, 411-416.

Brodersen, P., Petersen, M., Pike, H.M., Olszak, B., Skov, S., Odum, N., Jørgensen, L.B., Brown, R.E., and Mundy, J. (2002). Knockout of *Arabidopsis ACCELERATED-CELLDEATH11* encoding a sphingosine transfer protein causes activation of programmed cell death and defense. Genes Dev. *16*, 490-502.

Büschges, R., Hollricher, K., Panstruga, R., Simons, G., Wolter, M., Frijters, A., van Daelen, R., van der Lee, T., Diergaarde, P., Groenendijk, J., et al. (1997). The barley *Mlo* gene: a novel control element of plant pathogen resistance. Cell *88*, 695-705.

Chory, J., Peto, C.A., Ashbaugh, M., Saganich, R., Pratt, L., and Ausubel, F. (1989). Different roles for phytochrome in etiolated and green plants deduced from characterization of *Arabidopsis thaliana* mutants. Plant Cell *1*, 867-880.

Conklin, P. (2001). Recent advances in the role and biosynthesis of ascorbic acid in plants. Plant Cell Environ. *24*, 383-394.

Dietrich, R.A., Delaney, T.P., Uknes, S.J., Ward, E.R., Ryals, J.A., and Dangl, J.L. (1994). Arabidopsis mutants simulating disease resistance response. Cell *77*, 565-577.

Dietrich, R.A., Richberg, M.H., Schmidt, R., Dean, C., and Dangl, J.L. (1997). A novel zinc finger protein is encoded by the Arabidopsis *LSD1* gene and functions as a negative regulator of plant cell death. Cell *88*, 685-694.

Gray, J., Janick-Buckner, D., Buckner, B., Close, P.S., and Johal, G.S. (2002). Light-dependent death of maize *lls1* cells is mediated by mature chloroplasts. Plant Physiol. *130*, 1894-1907.

Greenberg, J.T., Guo, A., Klessig, D.F., and Ausubel, F.M. (1994). Programmed cell death in plants: A pathogen triggered response activated coordinately with multiple defense functions. Cell *77*, 551-563.

Hiraga, S., Sasaki, K., Ito, H., Ohashi, Y., and Matsui, H. (2001). A large family of class III plant peroxidases. Plant Cell Physiol. *42*, 462-468.

Hoisington, D.A., Neuffer, M.G., and Walbot, V. (1982). Disease lesion mimics in maize. 1. Effect of genetic background, temperature, developmental age, and wounding on necrotic spot formation with *Les1*. Dev. Biol. *93*, 381-388.

Hu, S.P., Zhou, Y., Zhang, L., Zhu, X.D., Li, L., Luo, L.J., Liu, G.L., and Zhou, Q.M. (2009). Correlation and quantitative trait loci analyses of total chlorophyll content and photosynthetic rate of rice (*Oryza sativa*) under water stress and well-watered conditions. J. Integr. Plant Biol. *9*, 879-888.

Huang, L., Sun, Q., Qin, F., Li, C., Zhao, Y., and Zhou, D.X. (2007). Down-regulation of a *SILENT INFORMATION REGULATOR2*-related histone deacetylase gene, *OsSRT1*, induces DNA fragmentation and cell death in rice. Plant Physiol. *144*, 1508-1519.

Ishikawa, A., Okamoto, H., Iwasaki, Y., and Asahi, T. (2001). A deficiency of coproporphyrinogen III oxidase causes lesion formation in Arabidopsis. Plant J. *27*, 89-99.

Johal, G.S., Hulbert, S.H., and Briggs, S.P. (1995). Disease lesion mimics of maize: A model for cell death in plants. Bioessays *17*, 685-692.

Kang, S.G., Jeong, H.K., and Suh, H.S. (2004). Characterization of a new member of the glutathione peroxidase gene family in *Oryza sativa*. Mol. Cells *17*, 23-28.

Kang, S.G., Matin, M.N., Bae, H.H., and Natarajan, S. (2007). Proteome analysis and characterization of phenotypes of lesion mimic mutant s*potted leaf 6* in rice. Proteomics *7*, 2447-2458.

Kato, N., and Esaka, M. (1999). Changes in ascorbate oxidase gene expression and ascorbate levels in cell division and cell elongation in tobacco cells. Physiol. Plant. *105*, 321-329.

Kim, J.A., Cho, K., Singh, R., Jung, Y.H., Jeong, S.H., Kim, S.H., Lee, J.E., Cho, Y.S., Agrawal, G.K., Rakwal, R., et al. (2009). Rice *OsACDR1* (*Oryza sativa* accelerated cell death and resistance 1) is a potential positive regulator of fungal disease resistance. Mol. Cells *28*, 431-439.

Kinoshita, T. (1995). Report of committee on gene symbolization, nomenclature and linkage groups. Rice Genet. Newsl. *12*, 9-115.

Lam, E., Kato, N., and Lawton, M. (2001). Programmed cell death, mitochondria and the plant hypersensitive response. Nature *411*, 848-853.

Liu, G., Wang, L., Zhou, Z., Leung, H., Wang, G.L., and He, C. (2004). Physical mapping of a rice lesion mimic gene, *Spl1*, to a 70-kb segment of rice chromosome 12. Mol. Gen. Genomics *272*, 108-115.

Mackinney, G. (1941). Absorption of light by chlorophyll solutions. J. Biol. Chem. *140*, 315-322.

Matin, M.N., Suh, H.S., and Kang, S.G. (2006). Characterization of phenotypes of rice lesion resembling disease mutants. Korean J. Genet. *28*, 221-228.

Matin, M.N., Pandeya, D., Baek, K.H., Lee, D.S., Lee, J.H., Kang, H., and Kang, S.G. (2010). Phenotypic and genotypic analysis of rice lesion mimic mutants. Plant Pathol. J. *26*, 159-169.

Mittler, R., Del Pozo, O., Meisel, L., and Lam, E. (1997). Pathogen-induced programmed cell death in plants, a possible defense mechanism. Dev. Genet. *21*, 279-289.

Mizobuchi, R., Hirabayashi, H., Kaji, R., Nishizawa, Y., Yoshimura, A., Satoh, H., Ogawa, T., and Okamoto, M. (2002). Isolation and

characterization of rice lesion-mimic mutants with enhanced resistance to rice blast and bacterial blight. Plant Sci. *163*, 345-353.
Morel, J.B., and Dangl, J.L. (1997). The hypersensitive response and the induction of cell death in plants. Cell Death Differ. *4*, 671-683.
Mori, M., Tomita, C., Sugimoto, K., Hasegawa, M., Hayashi, N., Dubouzet, J.G., Ochiai, H., Sekimoto, H., Hirochika, H., and Kikuchi, S. (2007). Isolation and molecular characterization of a *Spotted leaf 18* mutant by modified activation-tagging in rice. Plant Mol. Biol. *63*, 847-860.
Mosher, S., Moeder, W., Nishimura, N., Jikumaru, Y., Joo, S.H., Urquhart, W., Klessig, D.F., Kim, S.K., Nambara, E., and Yoshioka, K. (2010). The lesion-mimic mutant *cpr22* shows alterations in abscisic acid signaling and abscisic acid insensitivity in a salicylic acid-dependent manner. Plant Physiol. *152*, 1901-1913.
Nagato, Y., and Yoshimura, A. (1998). Report of the committee on gene symbolization nomenclature and linkage groups. Rice Genet. Newsl. *15*, 13-74.
Noutoshi, Y., Kuromori, T., Wada, T., Hirayama, T., Kamiya, A., Imura, Y., Yasuda, M., Nakashita, H., Shirasu, K., and Shinozaki, K. (2006). Loss of necrotic spotted lesions 1 associates with cell death and defense responses in *Arabidopsis thaliana*. Plant Mol. Biol. *62*, 29-42.
Pastori, G.M., Kiddle, G., Antoniw, J., Bernard, S., Veljovic-Jovanovic, S., Verrier, P.J., Noctor, G., and Foyer, C.H. (2003). Leaf vitamin C contents modulate plant defense transcripts and regulate genes that control development through hormone signaling. Plant Cell *15*, 939-951.
Persson, M., Falk, A., and Dixelius, C. (2009). Studies on the mechanism of resistance to *Bipolaris sorokiniana* in the barley lesion mimic mutant bst1. Mol. Plant Pathol. *10*, 587-598.
Qiao, Y., Jiang, W., Lee, J., Park, B., Choi, M.S., Piao, R., Woo, M.O., Roh, J.H., Han, L., Paek, N.C., et al. (2010). *SPL28* encodes a clathrin-associated adaptor protein complex 1, medium subunit micro 1 (AP1M1) and is responsible for spotted leaf and early senescence in rice (*Oryza sativa*). New Phytol. *185*, 258-274.
Ray, S., Anderson, J.M., Urmeev, F.I., and Goodwin, S.B. (2003). Rapid induction of a protein disulfide isomerase and defense-related genes in wheat in response to the hemibiotrophic fungal pathogen *Mycosphaerella graminicola*. Plant Mol. Biol. *53*, 741-754.
Rostoks, N., Schmierer, D., Mudie, S., Drader, T., Brueggeman, R., Caldwell, D.G., Waugh, R., and Kleinhofs. A. (2006). Barley necrotic locus *nec1* encodes the cyclic nucleotide-gated ion channel 4 homologous to the *Arabidopsis* HLM1. Mol. Genet. Genomics *275*, 159-168.
Schröder, E., and Pointing, C.P. (1998). Evidence that peroxiredoxins are novel members of the thioredoxin fold superfamily. Protein Sci. *7*, 2465-2468.
Simmons, C., Hantke, S., Grant, S., Johal, G.S., and Briggs, S.P. (1998). The maize lethal leaf spot 1 mutant has elevated resistant to fungal infection at the leaf epidermis. Mol. Plant Microbe Interact. *11*, 1110-1118.
Singh, K., Multani, D.S., and Khush, G.S. (1995). A new spotted leaf mutant in rice. Rice Genet. Newsl. *12*, 192-193.
Shin, S.Y., Kim, I.S., Kim, Y.H., Park, H.M., Lee, J.Y., Kang, H.G., and Yoon, H.S. (2008). Scavenging reactive oxygen species by rice dehydroascorbate reductase alleviates oxidative stresses in *Escherichia coli*. Mol. Cells *26*, 616-620.
Smirnoff, N. (1996). The function and metabolism of ascorbic acid in plant. Ann. Bot. *78*, 661-669.
Sugie, A., Murai, K., and Takumi, S. (2007). Alteration of respiration capacity and transcript accumulation level of alternative oxidase genes in necrosis lines of common wheat. Genes Genet. Syst. *82*, 231-239.
Tokunaga, T., and Esaka, M. (2007). Induction of a novel XIP-type xylanase inhibitor by external ascorbic acid treatment and differential expression of XIP-family genes in rice. Plant Cell Physiol. *48*, 700-714.
Tsunezuka, H., Fujiwara, M., Kawasaki, T., and Shimamoto, K. (2005). Proteome analysis of programmed cell death and defense signaling using the rice lesion mimic mutant *cdr2*. Mol. Plant-Microb Interact. *18,* 52-59.
Walker, M.A., and McKersie, B.D. (1993). Role of the ascorbate-glutathione antioxidant system in chilling resistance of tomato. J. Plant Physiol. *141*, 234-239.
Wang, F., Wang, G., Li, X., Huang, J., and Zheng, J. (2008). Heredity, physiology and mapping of a chlorophyll content gene of rice (*Oryza sativa* L.). J. Plant Physiol. *165*, 324-330.
Wei, X., Xu, J., Guo, H., Jiang, L., Chen, S., Yu, C., Zhou, Z., Hu, P., Zhai, H., and Wan, J. (2010). *DTH8* suppresses flowering in rice, influencing plant height and yield potential simultaneously. Plant Physiol. *153*, 1747-1758.
Wu, C., Bordeos, A., Madamba, M.R., Baraoidan, M., Ramos, M., Wang, G.L., Leach, J.E., and Leung, H. (2008). Rice lesion mimic mutants with enhanced resistance to diseases. Mol. Genet. Genomics *279*, 605-619.
Yamanouchi, U., Yano, M., Lin, H., Ashikari, M., and Yamada, K. (2002). A rice spotted leaf gene, *Spl7*, encodes a heat stress transcription factor protein. Proc. Natl. Acad. Sci. USA *99*, 7530-7535.
Yin, Z., Chen, J., Zeng, L., Goh, M., Leung, H., Khush, G.S., and Wang, G.L. (2000). Characterizing rice lesion mimic mutants and identifying a mutant with broad-spectrum resistance to rice blast and bacterial blight. Mol. Plant-Microbe Interact. *13*, 869-876.
Zeng, L.R., Qu, S., Bordeos, A., Yang, C., Baraoidan, M., Yan, H., and Xie, Q. (2004). *Spotted leaf11*, a negative regulator of plant cell death and defense, encodes a U-Box/Armadillo repeat protein endowed with E3 ubiquitin ligase activity. Plant Cell *16*, 2795-2808.